PB86-208576

Evolution of the Nocturnal Inversion Layer at an Urban and Nonurban Location

(U.S.) Environmental Sciences Research Lab.
Research Triangle Park, NC

1985

U.S. Department of Commerce
National Technical Information Service
NTIS

TECHNICAL REPORT DATA
(Please read Instructions on the reverse before comple

1. REPORT NO.	2.	3
EPA/600/J-85/427		PB86-208576

4. TITLE AND SUBTITLE	5. REPORT DATE
EVOLUTION OF THE NOCTURNAL INVERSION LAYER AT AN URBAN AND A NONURBAN LOCATION (Journal Version)	1985
	6. PERFORMING ORGANIZATION CODE
7. AUTHOR(S)	8. PERFORMING ORGANIZATION REPORT NO.
J. M. Godowitch, J. K. S. Ching, J. F. Clarke	
9. PERFORMING ORGANIZATION NAME AND ADDRESS	10. PROGRAM ELEMENT NO.
Same as block 12	CDWA1A/01-2144 (FY-84)
	11. CONTRACT/GRANT NO.
12. SPONSORING AGENCY NAME AND ADDRESS	13. TYPE OF REPORT AND PERIOD COVERED
Environmental Sciences Research Laboratory-RTP, NC Office of Research and Development U.S. Environmental Protection Agency Research Triangle Park, NC 27711	14. SPONSORING AGENCY CODE EPA/600/09

15. SUPPLEMENTARY NOTES

Ref: J. Climate & Appl. Meteorol., 24(8):791-804, August 1985

16. ABSTRACT

The evolutionary cycle of the nocturnal radiation inversion layer from formation until dissipation under fair weather conditions was investigated by time-series analyses of observations of inversion base and top heights, and inversion strength at an urban and a nonurban site in St. Louis, Missouri. The time-dependent behavior of each inversion parameter is presented from statistical and least-squares regression analyses. Differences of inversion evolution between these sites are discussed.

A surface-based inversion generally formed before sunset at the nonurban site and the growth of the inversion top height was described quite well by $(2K_T t)^{1/2}$, where K_T is the thermal eddy coefficient. The average time of formation of an elevated inversion layer at the urban site was 2.5 hours after sunset. The height of the nocturnal urban boundary layer decreased after formation under steady wind conditions.

The urban mixing height was consistently higher than that at the nonurban site during the morning, althouth the difference diminished with time since the nonurban mixing height growth rate was greater. The slower growth rate of the urban mixing height was attributed primarily to advection of relatively cold air and lower mixing heights from the upwind nonurban environment. A significant rise of the inversion top height at both sites after sunrise was attributed to urban-induced upward motions caused by low-level convergence that enhanced the observed mixing height growth rates.

17. KEY WORDS AND DOCUMENT ANALYSIS

a. DESCRIPTORS	b. IDENTIFIERS/OPEN ENDED TERMS	c. COSATI Field/Group

REPRODUCED BY
NATIONAL TECHNICAL
INFORMATION SERVICE
U.S. DEPARTMENT OF COMMERCE
SPRINGFIELD, VA. 22161

18. DISTRIBUTION STATEMENT	19. SECURITY CLASS (This Report)	21. NO. OF PAGES
RELEASE TO PUBLIC	UNCLASSIFIED	16
	20. SECURITY CLASS (This page)	22. PRICE
	UNCLASSIFIED	

EPA Form 2220-1 (9-73)

EPA/600/J-85/427
JOURNAL ARTICLE

Reprinted from JOURNAL OF CLIMATE AND APPLIED METEOROLOGY, Vol. 24, No. 8, August 1985
American Meteorological Society

Evolution of the Nocturnal Inversion Layer at an Urban and Nonurban Location

J. M. GODOWITCH,* J. K. S. CHING* AND J. F. CLARKE*

Meteorology and Assessment Division, Atmospheric Sciences Research Laboratory, Environmental Protection Agency, Research Triangle Park, NC 27711

(Manuscript received 4 July 1984, in final form 3 April 1985)

ABSTRACT

The evolutionary cycle of the nocturnal radiation inversion layer, from formation through the time of erosion under fair weather summer conditions was investigated by time-series analyses of observations of inversion base and top heights, and inversion strength at an urban and a nonurban site in St. Louis, Missouri. The time-dependent behavior of each inversion parameter is presented from statistical and least-squares regression analyses. Differences of inversion evolution between these sites are discussed.

A surface-based inversion generally formed before sunset at the nonurban site, and the growth of the inversion top height has been described quite well by $(2K_T t)^{1/2}$, where K_T is the thermal eddy coefficient. The average time of formation of an elevated inversion layer at the urban site was 2.5 h after sunset. The height of the nocturnal urban boundary layer decreased after formation under steady wind conditions.

The urban mixing height was consistently higher during the morning than at the nonurban site, although the difference diminished with time since the nonurban mixing height growth rate was greater. The slower growth rate of the urban mixing height was attributed primarily to advection of relatively cold air and lower mixing heights from the upwind nonurban environment. An overall rise of the inversion top height after sunrise was believed to be due to urban-induced upward motions, caused by low-level convergence that produced increasing mixing height growth rates. The average time for the inversion layer to erode completely was 4 h after sunrise at both sites.

1. Introduction

A surface-based radiation inversion layer is a common feature in temperature profiles at night in natural environments. In contrast, the nocturnal thermal structure in the highly inhomogeneous urban environment usually consists of an isothermal to adiabatic region, the urban boundary layer (UBL), which is capped by an elevated nocturnal inversion layer (NIL). The urban fabric is comprised of a variety of land uses, artificial surfaces and man-made structures that have different physical properties (e.g., thermal capacity and conductivity) than those of the surrounding natural environment. The vertical temperature structure of the UBL has been modified largely by an input of heat from underlying surfaces, buildings, and anthropogenic sources and also by downward transport of warmer air from the elevated inversion (Oke, 1982) as well as by mechanically-generated turbulence. However, the relative importance of these processes has been difficult to quantify.

While turbulent heat transfer and clear-air radiational cooling are the dominant processes governing the evolution of the nocturnal thermal structure in natural environments in the absence of large scale thermal advection and vertical motions, horizontal temperature gradients and vertical motions on the urban scale might also strongly influence the evolution of the UBL and urban NIL. Relatively large horizontal temperature gradients are established in the evening due to different cooling rates among the various land use areas in the urban region (Oke and Maxwell, 1975). Slower cooling rates at urban sites result in warmer temperatures relative to those in the nonurban surroundings (i.e., urban heat island). However, these spatial temperature differences decrease rapidly with height (Bornstein, 1968). Because of faster nonurban heating rates in the morning, horizontal temperature gradients often persist for a few hours after sunrise until the heat island is significantly reduced.

An urban region also has relatively high and unevenly distributed roughness features that contribute to a centripetal flow into the city when the airflow is very weak (Shreffler, 1978) or cause frictional retardation of the wind speed for stronger flows. These urban-induced modifications of the wind lead to convergence that produces upward motions within an urban area (Shreffler, 1979a). The relative importance of horizontal advection and urban-induced vertical motions on the evolution of the UBL and NIL needs to be explored. Better methods to treat the temporal and spatial variations of the vertical temperature structure during the morning period

* On assignment from the National Oceanic and Atmospheric Administration, U.S. Department of Commerce.

might lead to more accurate results in urban air-quality simulation models.

The primary emphasis herein is on the temporal behavior of the NIL at one urban and one nonurban location. The inversion parameters evaluated include the inversion base, strength, and inversion top. The height of the inversion base h, where the vertical temperature gradient (dT/dz) initially becomes positive, will denote the nocturnal UBL depth and the mixing height at both sites after sunrise. At the nonurban site, h was usually zero at night since the inversion was surface-based. The subscripts u and nu are used throughout this paper to distinguish between urban and nonurban observations, respectively. The inversion strength S represents the temperature difference between h and the inversion top height h_T, where dT/dz initially becomes negative. The nocturnal boundary layer (NBL) height where turbulence fluxes vanish often differs from h_T. Although flux profile measurements were not obtained during these experimental studies, Mahrt *et al.* (1979) found that the height of the nocturnal wind speed maximum h_j was at a level where turbulent fluxes disappeared. In this paper, the temporal variation of h_j at night is compared to the behavior of h_T. Other definitions for the NBL height are the vertical extent of significant cooling, and the height where the vertical temperature gradient becomes adiabatic. Heights from various definitions of the NBL have been compared elsewhere (Yu, 1978; Arya, 1981).

Time histories of observations of the inversion parameters at each site were evaluated with a least-squares quadratic regression in order to obtain best-fit curves. In addition, the time rate of change of h and h_T were analyzed statistically to assess the influence of various processes on inversion growth and erosion. In particular, it is believed that temporal variations in h and h_T after sunrise were strongly modulated by vertical motions and horizontal advection in the urban area. A significant rise of h_T often occurred after sunrise in St. Louis. The rate of change of h_T was evaluated to determine the impact of vertical motions on mixing height growth rates at these sites.

Thermal advection has been found to modulate strongly the sensible heat flux in an urban area (Ching *et al.*, 1983), which will influence the urban mixing height growth rate (Ching *et al.*, 1978). The relative effect of thermal advection on mixing height growth rates at both sites was examined by statistically analyzing the mixing height growth rates after removing vertical motions. Finally, the duration of the morning transition (i.e., the amount of time after sunrise for the nocturnal inversion to be completely eroded) was determined.

2. Experimental design and measurements

The data analyzed here were collected during an urban boundary layer field experimental program conducted in St. Louis, Missouri, as part of the Environmental Protection Agency's Regional Air Pollution Study (RAPS). The RAPS was designed to obtain a comprehensive data base of meteorological and pollutant measurements to assist in the development and evaluation of urban air quality models (Pooler, 1974). Schiermeier (1978) described the multitude of experimental studies undertaken during the RAPS. A major component of the UBL field program consisted of intensive experimental studies conducted during the evening and morning transition periods to document the spatial and temporal variations in the temperature structure during the development of the NIL after sunset and its erosion after sunrise the following morning.

Vertical temperature profiles were obtained by an instrumented helicopter during 31 evening and 46 morning experiments. These experimental studies were conducted over 5–6 week periods in July and August from 1974 to 1976. Most of the experiments were conducted under fair weather conditions with no clouds and with surface wind speeds of 1–3 m s^{-1}. However, during 11 experiments the cloud cover, as observed by the National Weather Service at Lambert-St. Louis Airport, was either broken or overcast at middle or high altitudes. Only the observations from 20 evening and 35 morning experiments conducted under clear skies are included in this paper.

The helicopter flights began about an hour before sunset (sunset was around 1900 local standard time) and usually ended by midnight. A morning experiment succeeded each evening experiment, although a greater number of morning experiments were conducted. Morning flights began shortly before sunrise (sunrise occurred around 0500 CST) and continued until there was no evidence of an inversion layer. This was determined in real time by a visual inspection of the temperature structure displayed on a chart recorder in the helicopter. On three occasions, flights commenced at midnight and continued after sunrise.

A typical flight plan consisted of a vertical sounding at each of several preselected sites located along a major highway coinciding as much as possible with the wind flow. Soundings were performed in counterclockwise ascent spirals from near ground level to 600 m or higher, if necessary. The ascent rate was about 2.5 m s^{-1} and a typical sounding required about four minutes.

Temperature measurements were obtained with a thermistor probe housed inside a cylindrical radiation shield and mounted ahead of the right helicopter skid. A forward speed of at least 20 m s^{-1} was maintained during a sounding to prevent possible interference to the measurements from helicopter rotor downwash. Altitude was obtained by a pressure altimeter that measured height above mean sea level (MSL) for a standard atmosphere. Time constants of the temperature and altitude sensors were 0.2 and

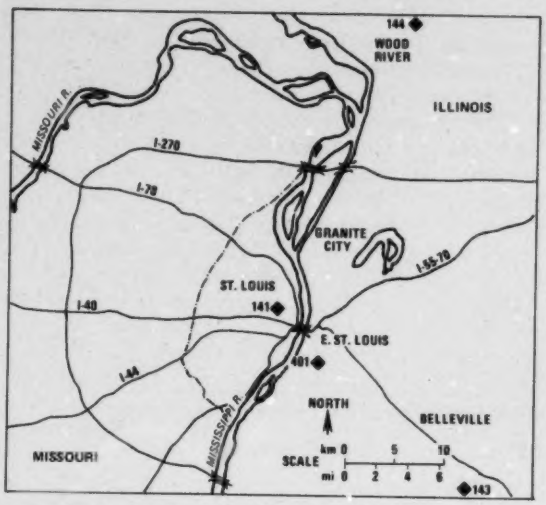

FIG. 1. Map of metropolitan St. Louis, MO shows the city limits (dot-dashed line) and the locations of the urban (141) and nonurban (401) sites. Other location numbers denote Upper Air Sounding Network (UASN) pibal and radiosonde sites.

0.02 s, respectively, and the relative accuracies were ±0.2°C and ±5 m.

Data were recorded on both digital and analog recorders. Analog charts provided continuous traces of temperature and altitude in each sounding during the entire program. During the 1975–76 experiments a digital data logger sampled at 2.5 s^{-1} to provide a vertical resolution of 1 m. Digitized records of the analog charts from the 1974 experiments and the digitally recorded data from the 1975–76 experiments were block averaged over 30 m intervals. Thus, small-scale fluctuations were effectively removed, yet sufficient resolution remained in the averaged profiles to permit an evaluation of the vertical temperature structure. The elevation above sea level of each site was subtracted from the altitude data to obtain heights above ground (AGL). The observations of h and h_T were resolved to the nearest 5 m and S was determined to within 0.1°C from nonaveraged temperature profiles.

During each intensive study period, wind speed and direction profiles were obtained hourly by tracking pilot balloons (pibals) with a single theodolite. The pibal wind measurements had a vertical resolution of approximately 80–90 m. Interpolated values at 50 m intervals were derived by a cubic spline interpolation method. The height of the nocturnal wind speed maximum was obtained from the interpolated wind profiles.

3. Site description

The St. Louis metropolitan area is shown in Fig. 1. The downtown area is situated along the west bank of the Mississippi River. The population within the city limits is approximately 622 000, and the surrounding metropolitan area, which includes numerous communities on both sides of the river, has a population of 2.4 million. The topography is relatively flat in the region; however, the terrain slopes upward from the river toward the west. Elevation varies from 122 m MSL at the river to 180 m MSL approximately 20 km west of the downtown center. An extensive low-lying flat area known as the American Bottoms extends approximately 15 km east of the river at an average elevation of 128 m MSL. More details about the geographic features and a topographic contour map of the St. Louis region are given in Hjelmfelt (1982).

The observations in this paper were obtained at the two principal sounding sites of the UBL field program. The locations of these sites are denoted on the map in Fig. 1. The urban site (141) was situated in a commercial and multiple story building district approximately 3 km west of the downtown center. The nonurban site (401) was approximately 7 km southeast of the city at Bi-State Parks airport, which was also used as the base of operations for helicopter flights. Land use in the immediate area, in sharp contrast to that at the urban site, included forested tracts and agricultural cropland surrounding the grass-covered land at the airport. However, because of the relatively large and variable roughness features and differing land use in the vicinity, the nonurban site was not an ideal homogeneous location. More detailed descriptions of the various land uses and a land use map of the St. Louis region are provided by Auer (1978). Generally, 5–8 profiles were obtained at each site during an experiment. Since soundings were also performed at several other sites during a flight, the interval between profiles at a site varied from 30 to

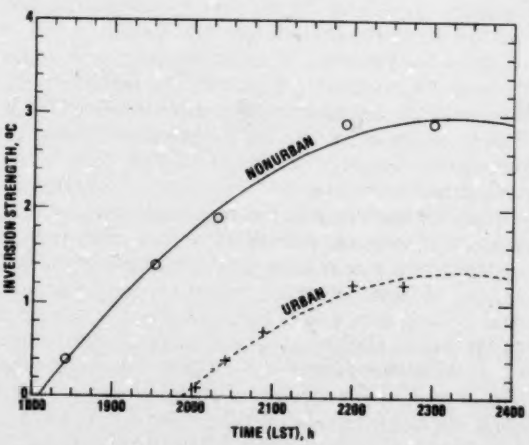

FIG. 2. Temporal variation of inversion strength (S) on 19 August 1974. The evolution of S at each site is from a least-squares quadratic regression fit of the observations. Sunset occurred at 1850 CST.

45 minutes. A sounding began at the ground at the nonurban site and from 30–50 m above the urban surface because of buildings and other obstructions in the vicinity.

4. Inversion formation

The time of formation of the nocturnal inversion is dependent upon the ability of the air to cool; which is greatly influenced by meteorological conditions and the physical characteristics of a surface (e.g., thermal capacity, thermal conductivity). Clear, dry and light wind conditions are conducive to rapid cooling of the ground by longwave radiation. This leads to the formation of a surface-based inversion in nonurban locations by sunset. In an urban area, where the higher and more uneven roughness features produce greater mechanical mixing and the man-made surfaces and building materials readily conduct and store heat by day and release large amounts in the evening, surface inversions are rare. Instead, an elevated inversion layer develops and has been observed above the UBL before midnight (Duckworth and Sandberg, 1954; Ackerman *et al.*, 1981).

An examination of temperature profiles revealed that the nonurban surface-based and urban elevated inversions formed at considerably different times. It was difficult to estimate the time of inversion formation by inspection of the evening temperature profiles because of the relatively large time interval between profiles. Therefore, in an effort to more accurately determine the time of inversion formation t_f, the time series of S observations were evaluated. A typical case study (Fig. 2) shows the temporal behavior of S during a clear evening to be similar at both sites. The time when S becomes nonzero was defined as t_f. It is evident in Fig. 2 that nonurban inversion formation occurred earlier and S was significantly greater at the nonurban site. Analogous results were found in the other case studies.

Generally, S evolved in a nonlinear manner and a quadratic regression equation usually described the temporal behavior quite well, as demonstrated by the close fit of the curves to the observations in Fig. 2. The best-fit regression equation of each time series was solved for the time when S was zero. A sufficient number of observations for regression analysis was obtained at both sites during 20 evening experiments. In a few cases a regression curve inadequately fit the observations because of variations in the evolution of S, so t_f was found by a subjective evaluation of the time series. The difference between t_f and the time of sunset was determined and the results are given in Table 1. The number of cases of inversion formation were grouped into one hour intervals before or after sunset.

TABLE 1. Frequency of inversion formation.

	Hour interval from sunset					
	(−2)–(−1)	(−1)–(0)	0–1	1–1	2–3	3–4
Nonurban	5	14	1	—	—	—
Urban	—	—	4	8	5	3

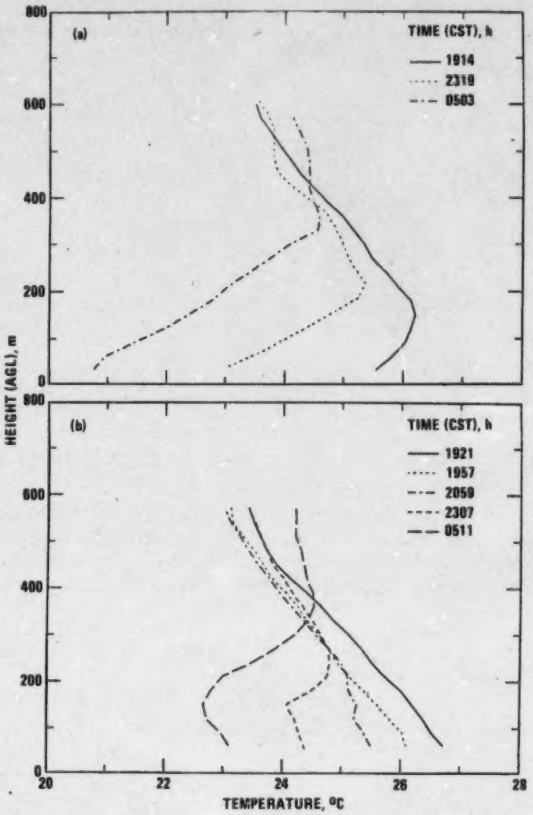

FIG. 3. Temperature profiles at the a) nonurban and b) urban sites on 26–27 July 1975. Sunset and sunrise were at 1917 and 0458 CST.

In 19 of 20 cases an inversion formed before sunset at the nonurban site. Nonurban inversion formation occurred most frequently within the one-hour period before sunset, although in 25% of the cases an inversion was established even earlier. The average time of formation was 0.5 h before sunset. In all cases, the nonurban inversion was surface based. These results were also consistent with those of more ideal remote sites where presunset inversion formation is a common occurrence over the annual cycle (e.g., DeMarrais, 1961; Takle *et al.*, 1976).

In contrast, the results in Table 1 for the urban site show that t_f was always after sunset and more variable than at the nonurban site. The average t_f at the urban site from these summer experiments was

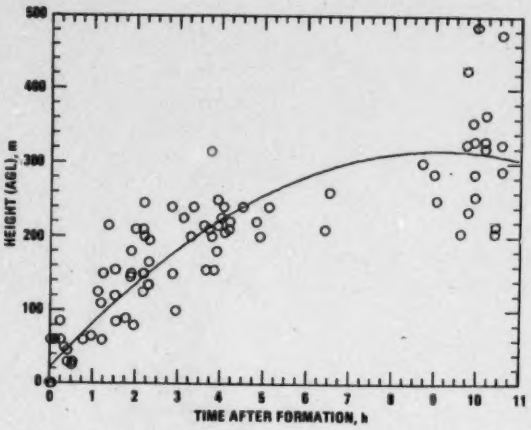

FIG. 4. Observations of the inversion top (h_T) at the nonurban site from 20 summer experiments. The h_T growth curve was derived by a least-squares quadratic regression fit of the observations. The coefficient of correlation (r) was 0.91 and the standard error of estimate was 80.5 m.

2.5 h after sunset, although individual values ranged from 1.0 to 4.0 h after sunset. Inversion formation statistics derived from temperature difference measurements on a 152 m tower in St. Paul–Minneapolis by Baker *et al.* (1969) also displayed large variability in t_f. However, their results for the midsummer months revealed that an elevated inversion formed most often at midnight. At formation, the elevated inversion in St. Louis was a thin layer and its base was often higher than 150 m. The difference from our experimental results might be explained by the inversion forming above the tower and its base eventually descending.

A comparison of individual urban and nonurban results revealed that the urban inversion had indeed formed later in all cases, with an average difference of nearly 3 h. The near-adiabatic thermal structure at the urban site around sunset suggests that mixing was still relatively active, whereas at the nonurban site stable conditions had already been established. Evidence from temperature profiles at various sites across the city indicated that the surface inversion layer was eroded from below as it moved across the relatively warm, rougher urban environment. The elevated inversion at the urban site generally formed when h_T at the nonurban site was at 150–200 m. The variability in t_f at the urban site was attributed to differences in wind speed and direction, distance from the upwind edge of the urban area (which varied with direction because of the metropolitan area's asymmetric shape), and variability in the growth rate of the nonurban inversion layer. These factors appeared to govern the time of formation of the urban inversion in a complicated manner that would make t_f difficult to predict.

5. Inversion development at night

The temperature profiles in Fig. 3 depict the typical evolution of the thermal structure at both sites. Considerable cooling occurred up to 150 m by 1914 CST at the nonurban site (Fig. 3a). Subsequent profiles show that S and h_T increased with time as the nonurban inversion extended to 300 m by sunrise. The temperature profiles at the urban site (Fig. 3b) show the evolution of an elevated inversion layer and UBL.

This section describes the nocturnal evolution of the inversion layer at both sites and the temporal variation of the UBL height at the urban site.

a. Nonurban

Individual time histories showed that h_T continually increased overnight, in agreement with other experimental results (e.g., Mahrt *et al.*, 1979; Yamada, 1979). The observations for all experiments and the class average time variation of h_T, as derived from a least-squares quadratic regression fit, are shown in Fig. 4. The growth curve for h_T is given by

$$h_T = 21.5 + 64.6t - 3.5t^2, \qquad (1)$$

where t represents time in hours after formation. A nonzero h_T exists when t is zero in Eq. (1). When h_T is set to zero, the average time of formation occurs only one-third of an hour earlier than the average value indicated in the previous section. Thus, Eq. (1) does not adequately model the initial growth of h_T. Nevertheless, Eq. (1) describes the overall evolution of h_T quite well because the growth of h_T in individual cases also exhibited a similar nonlinear time dependence.

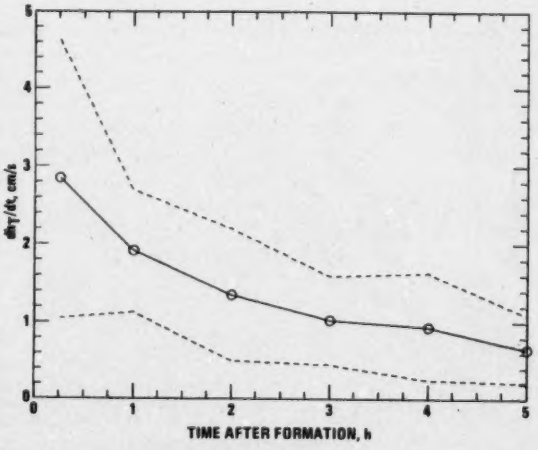

FIG. 5. Temporal variation of the inversion top growth rate (dh_T/dt) at the nonurban site. Dashed lines represent one standard deviation from the hourly averaged values.

The pattern of growth exhibited by the observations in Fig. 4 indicated that the growth rate of the inversion top dh_T/dt decreased with time. When Eq. (1) is differentiated by t, the average growth rate of h_T decreases linearly with time according to

$$dh_T/dt = 64.6 - 7.0t, \qquad (2)$$

where the growth rate has units of m h^{-1}.

The temporal behavior and variability of dh_T/dt were further investigated by computing individual growth rates between consecutive observations. The time assigned to each dh_T/dt was the average time between observations. Hourly averaged growth rates were computed from the individual values, and an initial inversion growth rate was determined from values within 30 min after formation. The results (Fig. 5) showed that h_T growth was extremely rapid and more variable immediately after formation, as dh_T/dt was nearly 3 cm s^{-1} (i.e., about 100 m h^{-1}). Hence, the initial growth rate is underestimated by Eq. (2). The growth rate of h_T steadily decreased both on average and for individual case studies. The variability of dh_T/dt is depicted in Fig. 5 by the dashed lines representing one standard deviation from the average values. Although the growth rate of h_T could not be determined on an hourly basis after midnight, h_T growth was even more gradual during the period after midnight, with an average dh_T/dt of 0.5 cm s^{-1} derived from observations at midnight and sunrise.

Figure 6 depicts inversion growth after the observations for each case were scaled by the value at sunrise. These results also demonstrate that inversion growth was more rapid before midnight. In most cases, h_T attained about two-thirds of its final height at sunrise within 3–4 h after formation. The standard error of estimate indicated scatter on the order of

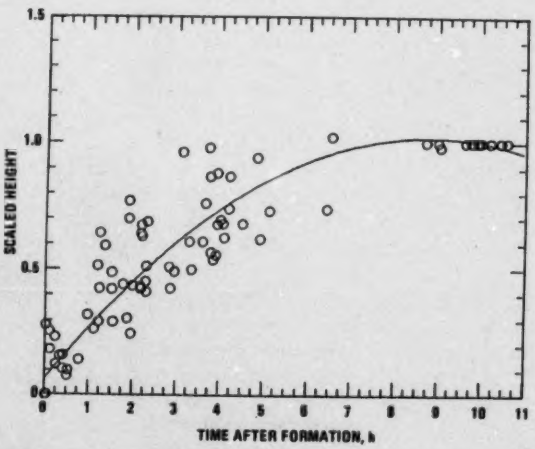

FIG. 6. Observations of the nonurban inversion top scaled by h_T at sunrise.

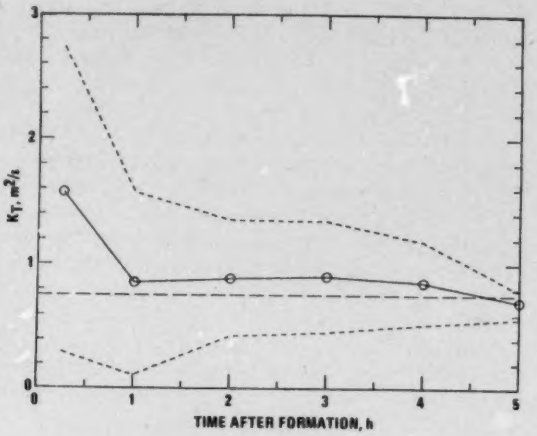

FIG. 7. Variation of the hourly averaged thermal eddy coefficient K_T (O) and its standard deviation (dashed lines) during the evening. The long dashed line is $K_T = 0.75$.

10–15% from the regression curve in Fig. 6. These results also show that on the average, h_T increased in an orderly manner overnight.

Since the growth rate of h_T in Fig. 5 exhibits an inverse square root of time variation, the applicability of the evolution of h_T following a $t^{1/2}$ curve was examined. An inversion growth formula developed by Taylor (1915) that describes the development of the top of a cooled layer of relatively warm land-based air as it travels over a cold water body is given by

$$h_T = 2(K_T t)^{1/2}, \qquad (3)$$

where K_T is a bulk thermal eddy coefficient and t the amount of time since inversion formation. Equation (3) has also been applied to inversion growth over land. Anfossi *et al.* (1974) and Kloppel *et al.* (1978) found that a constant K_T of 0.3 m^2 s^{-1} in Eq. (3) simulated the growth of h_T under clear, calm conditions as h_T reached a height of about 200 m by sunrise.

The evolution of h_T was assumed to follow the square root of time dependence given by Eq. (3) and h_T observations at sunrise were used to determine K_T. Since h_T at the nonurban site varied from 210–480 m at sunrise, individual values of K_T ranged from 0.28–2.0 m^2 s^{-1}. However, a K_T of 0.75 m^2 s^{-1} was found to predict the average value of h_T at sunrise.

Additional analysis was performed with all observations to determine whether a temporally constant K_T accurately simulated the evolution of h_T. The results (Fig. 7) showed that, after an initially large value, K_T was nearly constant at 0.9 from 1–4 h after formation. Thus, on an average, K_T was larger during the evening period than at sunrise. However the standard deviations, denoted by dashed lines in Fig.

7, revealed that K_T was likely to vary by about a factor of 2 for any given hour before midnight.

Figure 8 depicts the growth of h_T from Eq. (3) with K_T = 0.75, and the temporal variation of h_j derived from wind profiles at sites 141 and 143 on the nights of experiments. A wind speed maximum became well-defined aloft about an hour after sunset and its magnitude increased rapidly until midnight. Oscillations of h_j were observed from hour to hour. However, in the mean, h_j remained relatively constant and gradually descended somewhat before sunrise, while h_T continually increased overnight. A notable feature in Fig. 8 is that h_j at site 143 became less than h_T around midnight, although the time of this occurrence varied from case to case. Mahrt *et al.* (1979) also showed that h_j was less than h_T and h_j remained relatively constant or even decreased overnight.

Another interesting feature in Fig. 8 is the greater height of the wind speed maximum at the urban site, even though h_T was about the same height at both sites. Moses (1974) also reported that h_j was higher at urban sites from pibal measurements in St. Louis during the METROMEX program. On average, h_j was slightly higher than h_T, which indicates the potential for greater instability at this urban site than in the nonurban area. Nevertheless, h_j at the urban site was also less than h_T by sunrise with no evidence that an inversion breakup had occurred.

The temporal behavior of S is displayed by scaled observations in Fig. 9. As noted earlier, S continually increased overnight and an overall square root of time dependence is evident in these results. Hence, S initially increased rapidly and then its rate of change slowly diminished with time. Stull (1983) reported a similar temporal behavior for the near-surface temperature strength, which he defined as the amount of cooling since inversion formation.

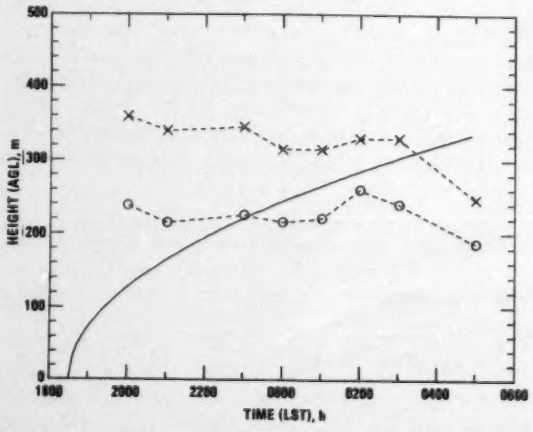

FIG. 8. Evolution of the nonurban h_T from Eq. (3) with K_T = 0.75 m^2 s^{-1} and the temporal variation of the height of the nocturnal wind speed maximum (h_j) at the urban site (×) and at site 143 (○).

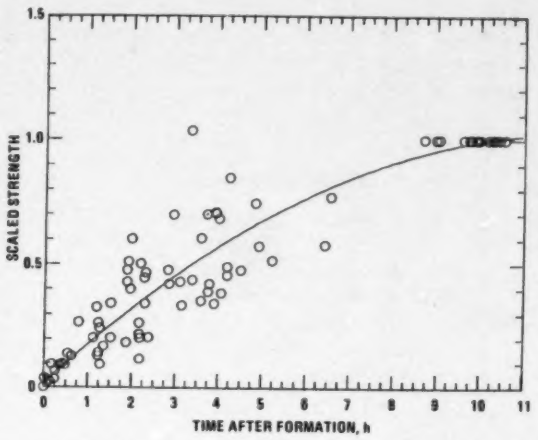

FIG. 9. Temporal variation of the nonurban inversion strength scaled by S at sunrise.

b. Urban

Knowledge of h_u and its temporal variation at night are important for urban dispersion modeling, as surface-released pollutants are generally uniformly distributed in the UBL. Large decreases in aerosol concentrations were found near h_u (Godowitch, 1982). Observations of h_u in Fig. 10a were scaled by the value at sunrise and because of the large variation in t_f, the time of an observation after t_f was scaled by the amount of time from formation to sunrise. Nevertheless, no clearly defined pattern emerged for the early evolution of h_u. At formation, h_u ranged from about 0.5–2.5 times its height at sunrise. However, upon closer examination, h_u decreased with time on most nights. In the cases when h_u was shallower before midnight than at sunrise, the wind flow had gradually shifted overnight to a direction that increased the distance to the upwind edge of the urban area.

This behavior in h_u was observed during the experimental program when winds changed from southeast to southwest. It is believed, therefore, that h_u increased in part because of the longer urban fetch toward the southwest. However, under steady wind flow conditions, h_u is expected to decrease after formation because of a gradual reduction of the heat flux in the urban area, coupled with an increase in the thermal stratification of the upwind surface inversion. The largest variations of h_u, however, occurred within a few hours after formation. Observations obtained from experiments which started at midnight showed h_u to be nearly constant between midnight and sunrise. Nevertheless, these results suggest that a constant value would not be representative of h_u before midnight or under temporally varying

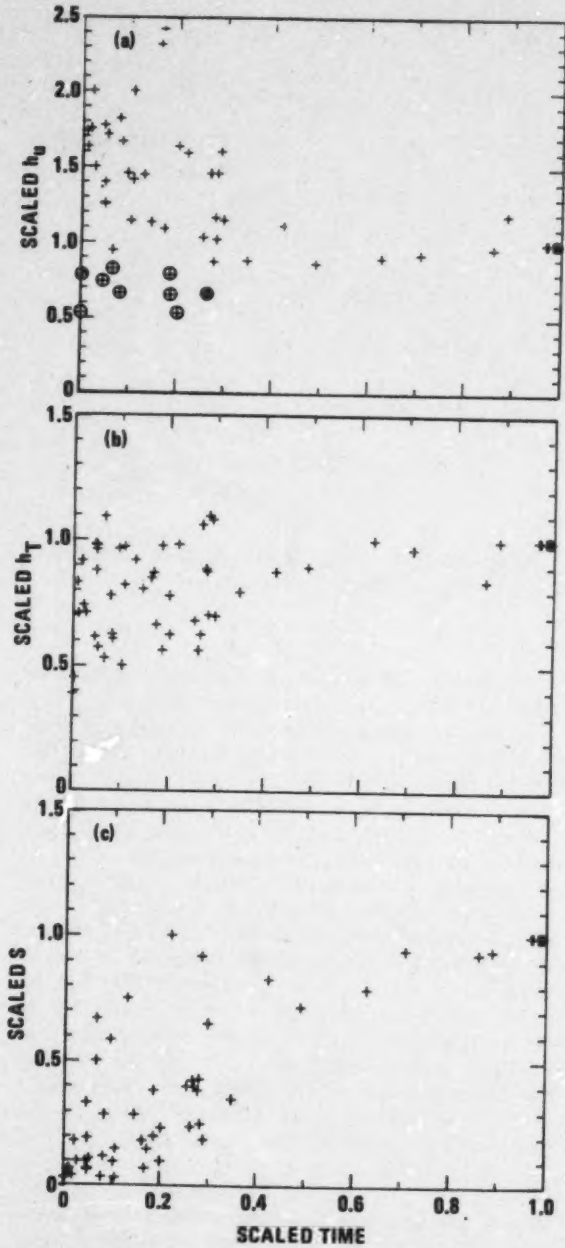

FIG. 10. Temporal variation of a) UBL depth (h_u), b) urban inversion top (h_T) and c) urban inversion strength S each scaled by values at sunrise. The time of an observation after formation was normalized by the interval between formation and sunrise. Circled h_u observations were taken on evenings when the wind direction shifted.

wind flows at night. Detailed analyses of vertical time sections of temperature by Ackerman *et al.* (1981) also showed variations in h_u overnight.

Figure 10b contains the scaled urban h_T observations. At formation, h_T varied from 0.5 to 1.2 times its height at sunrise. The urban h_T increased gradually with time in the same manner as h_T at the nonurban site. Since h_u generally descended, the urban inversion became thicker overnight.

The scaled S observations at the urban site in Fig. 10c show a continual and orderly increase in S, except in a few cases when the inversion was very weak all night (i.e., $S < 0.5$°C). As noted earlier, S was always smaller in the urban inversion, but its temporal behavior was similar at both sites.

6. Statistics and structure of the nocturnal inversion at sunrise

Observations of the inversion parameters at the relatively steady-state period around sunrise were statistically analyzed to establish the initial conditions of the inversion layer at both sites. A single elevated inversion layer was typically observed at the urban site, whereas a surface-based inversion still existed at the nonurban site.

Statistics in the form of means and standard deviations of various inversion parameters from 35 cases are presented in Table 2. The mean h_u was 150 m; however, the minimum and maximum values differed by a factor of 5. The mean nonurban S was 2.5 times greater than S at the urban site, and individual observations of S at these sites were positively correlated. The height of h_T was nearly the same at both sites, both on an average and an individual basis. The inversion gradient γ, the vertical temperature gradient from the base to h_T, was greater in the nonurban inversion.

The urban statistics in Table 2 are site-specific under these conditions. Several factors, such as city size, wind speed, upwind inversion gradient and distance of a site from the upwind edge of the city, influence h_u and S. Summers (1965) incorporated these variables into a thermodynamic model that describes the development of h_u. Results of several urban studies (e.g., Bornstein, 1968; Clarke, 1969; Oke and East, 1971) have essentially supported the parameterization of the Summers model on the up-

TABLE 2. Statistics of the inversion parameters at sunrise.

Site	Statistic	h (m)	S (°C)	h_T (m)	γ (°C/km)
Urban	Mean	150	1.8	325	10.3
	Standard deviation	±57	±0.8	±103	±3.5
	Range	60–310	0.2–4.4	185–605	3.5–19.5
Nonurban	Mean	0.0	4.4	335	14.5
	Standard deviation	—	±1.4	±86	±6.2
	Range	—	1.5–6.6	185–605	6.6–23.2

wind side of a city for other than calm wind conditions. Statistics for New York City (Bornstein, 1968), which is considerably larger than St. Louis in horizontal and vertical extents, show an average h_u about twice that for this urban site, while the average S was about the same. Thus, areal size and the vertical dimension of a city are important factors that determine the maximum height of the nocturnal UBL. Consequently, a shallower average UBL is expected in smaller cities, as observed in Cincinnati, Ohio (Clarke, 1969) and Columbus, Ohio (McElroy, 1973) where h_u was typically 100 m or less in the downtown area.

Inversion parameters at a specific site are also influenced by the site's location relative to the upwind edge of the urban area, which usually varies with direction because of the complex shape of most cities. The directional dependence of the inversion parameters was examined by grouping the observations into four 90° quadrants centered on the northeast, southeast, southwest and northwest. A layer-average wind direction from the surface to h_T was derived from pibal wind profiles. In most cases the wind flow up to h_T was within one quadrant. In no cases were winds from the northwest. The results for both sites for three wind direction quadrants are shown in Table 3. The results of the southeast and southwest quadrants are more statistically reliable since 14 and 16 cases were found for these quadrants, respectively.

Several notable differences in the inversion parameters were apparent between the southeast and southwest quadrants. Results for the urban site indicate that h_u was shallower, S was smaller, and h_T was considerably lower for southeast flows. The average h_u for the southwest quadrant was about 50 m higher than for the southwest quadrant. This difference might be due to a combination of a weaker inversion gradient in the nonurban inversion and the longer distance of urban land use in the southeast quadrant. In addition, southwest flows were distinguished from the other wind regimes by stronger and higher jets which were associated with thicker inversions. This was evident in the urban results for the southwest cases. The nonurban inversion was slightly influenced by the urban area under southwest flows, particularly under the more westerly flows, as the average S was greater under southeast flows at this site.

TABLE 3. Directional dependence of the inversion parameters.

Direction	h (m)	S (°C)	h_T (m)	γ (°C/km)	N
		Urban			
Northeast	143 ± 36	1.0 ± 0.3	274 ± 55	7.8 ± 2.4	5
Southeast	123 ± 36	1.6 ± 0.6	283 ± 58	10.4 ± 3.2	14
Southwest	175 ± 66	2.4 ± 0.9	386 ± 115	12.2 ± 3.6	16
		Nonurban			
Northeast	0.0	3.7 ± 1.2	315 ± 28	11.8 ± 4.2	5
Southeast	0.0	5.1 ± 1.2	306 ± 67	17.8 ± 6.2	14
Southwest	0.0	4.0 ± 1.4	390 ± 100	11.0 ± 3.4	16

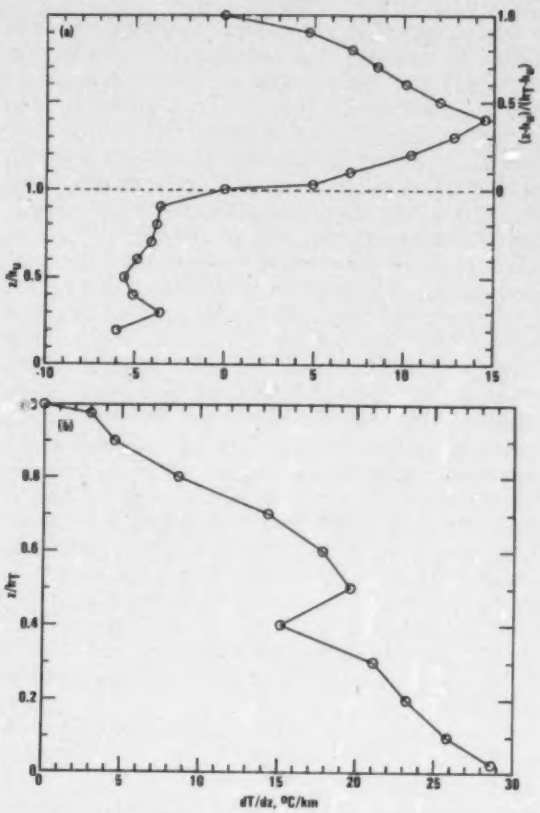

FIG. 11. Scaled profiles of the vertical temperature gradient (dT/dz) at the a) urban and b) nonurban sites.

The temperature profiles reveal that γ did not represent the vertical structure everywhere within the inversion, so the variation of the thermal structure was investigated by computing the vertical temperature gradient dT/dz from temperatures averaged over 30 m intervals. Height z at the nonurban site was scaled by h_T. Individual profiles of dT/dz showed that the strongest thermal stratification existed near the ground. However, the variability in dT/dz was also largest near the surface. An interesting feature common to most of the profiles was a gradual decrease in dT/dz in the lower half of the inversion, which indicates that temperature did not increase linearly with height. An elevated peak in dT/dz was found at $0.6 \pm 0.1 h_T$ and the average dT/dz at this level was 24.5°C km^{-1}. In a few cases, when dT/dz decreased monotonically through the inversion layer, no distinct wind maximum was observed and wind speeds were very light within the inversion layer.

An average dT/dz was computed at $0.1h_T$ intervals within the inversion. The nonurban profile of average dT/dz in Fig. 11b displays the same features exhibited by the individual profiles. Thermal gradients were greatest in the lower half of the inversion. Moreover, averages and their standard deviations (not depicted) were about the same size up to $0.4h_T$. The magnitude of dT/dz at the elevated peak was slightly smaller than that found earlier, and occurred at $0.5h_T$. This was a result of the averaging process since the peak gradient occurred at different heights. A comparison of the height of the elevated peak gradient and h_j at site 143 showed that both were about the same level within the resolution of the pibal measurements. Mahrt *et al.* (1979) showed that turbulence fluxes vanished just below h_j. It is reasonable that the jet would be situated at a level of minimal turbulence where the temperature structure exhibits strong stability. Above the elevated peak in Fig. 11, dT/dz decreased dramatically in the upper part of the inversion. Andre and Mahrt (1982) reported turbulence transport to be more important to temperature evolution in the lower part of the inversion layer and clear-air radiational cooling to be the dominant factor in the upper part of the inversion layer where stability is weaker. Their findings appear to be supported by these results.

A composite profile of the overall thermal structure at the urban site is presented in Fig. 11a. It shows a wide variation in thermal stability at this location. The temperature structure in the UBL was determined by scaling z by h_u and the structure of the inversion layer was derived by scaling the difference between z and h_u by the inversion thickness ($h_T - h_u$). Temperature gradients in the UBL were about $-5°C\ km^{-1}$ which are comparable to $-6°C\ km^{-1}$ in the UBL over Montreal (Yap *et al.*, 1969). Thus, the thermal structure below h_u was more stable at sunrise than during the evening when temperature gradients were near-adiabatic. In addition, the results in Fig. 11 reveal that dT/dz increased with height within the UBL. Entrainment between the UBL and inversion is a likely mechanism for the modification of the thermal structure near h_u. Thermal stability increased dramatically above h_u to a maximum near the middle of the inversion layer. In the upper part of the inversion, dT/dz decreased rapidly up to h_T in the same manner as in the nonurban inversion. Clearly, the largest differences in dT/dz between these sites existed below the height of the midpoint of the inversion where urban effects strongly influenced the vertical temperature structure.

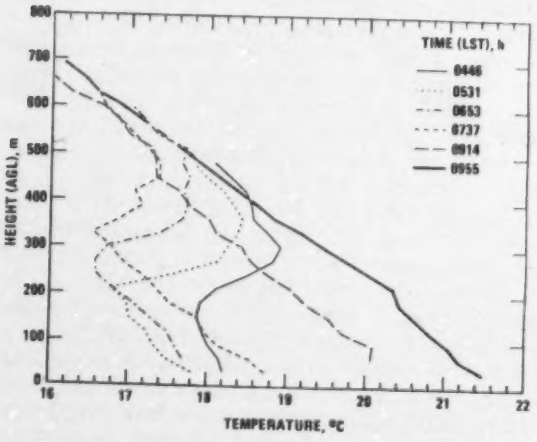

FIG. 12. Temperature profiles at the urban site on 3 August 1976. Sunrise occurred at 0503 LST.

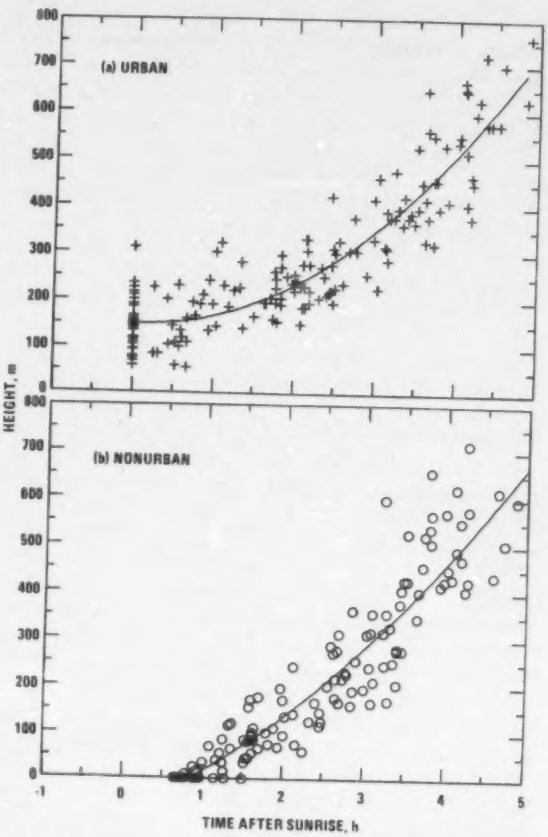

FIG. 13. Mixing height observations at the a) urban and b) nonurban sites. Urban (h_u) and nonurban (h_{nu}) mixing height growth curves were derived from a least-squares quadratic regression fit of each data set.

7. Erosion of the nocturnal inversion layer

A typical set of profiles from a single experiment in Fig. 12 illustrate the evolution of the temperature structure after sunrise at the urban site. A notable

feature is cooling below h_u in the profiles obtained within 2 h after sunrise. During this time the urban heat island was still strong, and significant horizontal temperature gradients existed across the urban area. The urban site was situated upwind of the center of the heat island because of easterly winds during this particular morning, which subjected this site to cold air advection. Temperatures below h_u in the profile at 0653, obtained nearly 2 h after sunrise, were lower than those in the profile near sunrise. It is apparent that advection of cold air was not matched by local sensible heating during this time. Similar results were displayed by urban profiles in the other cases. The nonurban site, on the other hand, should not be affected by thermal advection; an examination of sets of nonurban profiles revealed that advective effects were indeed undetectable.

The urban profiles in Fig. 12 also exhibit appreciable rises in h_u and h_T during the morning period. While h_u was expected to increase due to convective turbulence and heating, the large rise in h_T cannot be explained by convective processes. Note that the temperature change from one h_T to another in Fig. 12 can be closely approximated by following an adiabat from the temperature at h_T earlier. Hence, the rise of h_T is believed to be caused by urban-induced upward motions that require an adiabatic cooling when lifting occurs. Time series of convergence derived from minute-averaged winds measured at 30 m from a network of towers surrounding the urban site suggest that vertical motions do exist in St. Louis (Shreffler, 1979a). Those results and the results of Shreffler (1979b), which reveal slower wind speeds in urban locations due to frictional retardation, support an explanation that the inversion layer was lifted by upward motions when coupled with increasing instability during the morning. During the night, convergence was small because of strong thermal stability associated with the elevated inversion. Thus, sensible heating, advection, and vertical motions can occur concurrently to influence the temporal behavior of the inversion layer after sunrise. The pattern of evolution of each inversion parameter and the relative influence of these processes on inversion erosion were explored.

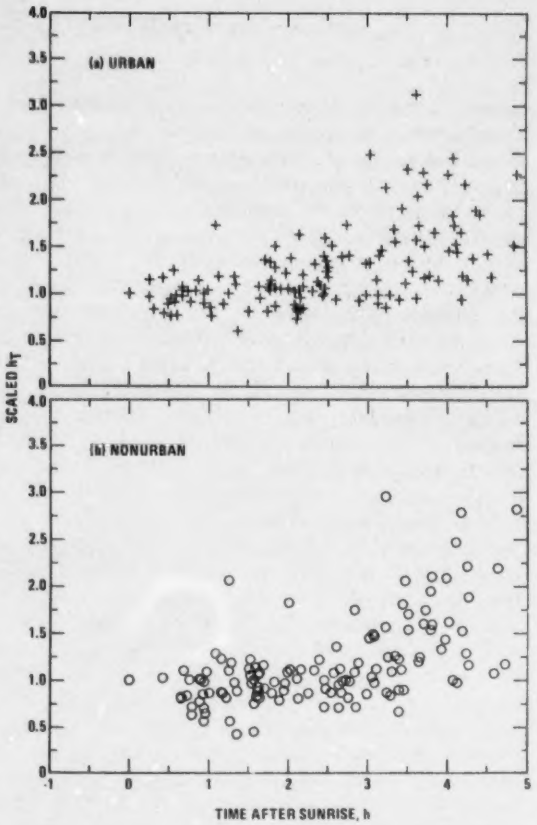

FIG. 15. Inversion top observations at the a) urban and b) nonurban sites are scaled by h_T at sunrise.

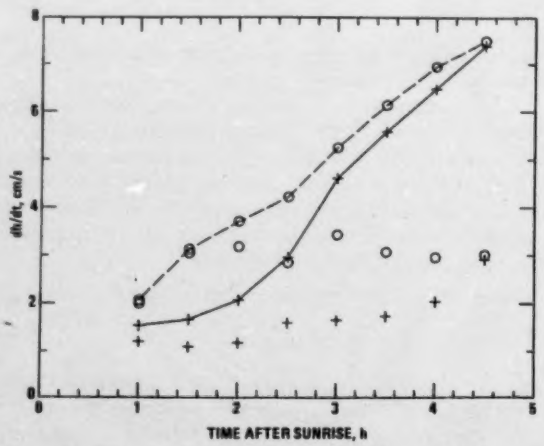

FIG. 14. Mixing height growth rate (dh/dt) averaged over one-hour intervals at the urban (pluses) and nonurban (circles) sites. Relative growth rates, after h_T variations were removed, are denoted by unconnected symbols.

Mixing height observations at the urban and nonurban sites are displayed in Fig. 13. Large variations in mixing height are expected in time and space during the highly turbulent and nonstationary period after sunrise. These variations are exacerbated by differences in meteorological factors among the cases. However, individual time histories of h_u and h_{nu} indicated that the mixing height evolved in a parabolic manner at both sites. The mixing height growth curves in Fig. 13 were obtained by a least-squares quadratic regression fit of the observations and are given by

$$h_u = 150.0 - 7.0t + 24.3t^2, \quad (4)$$

$$h_{nu} = -56.3 + 57.1t + 18.5t^2, \quad (5)$$

where t is time in hours after sunrise. Clearly, the t^2 term becomes dominant as the morning progresses. According to Eq. (5), nonurban mixing layer growth begins about 45 min after sunrise, although h_{nu} was often observed to be zero for over an hour after sunrise. The goodness of fit is given by a coefficient of correlation, r, which was 0.91 and 0.92 for the urban and nonurban results, respectively. Some of the scatter at the nonurban site was attributed to sampling variability since the observations were instantaneous rather than time-averaged values.

At sunrise, h_u was 150 m higher than h_{nu} on average. However, the difference between mixing heights at these sites, as derived from the growth curves, diminished with time, indicating that the growth rate of h_{nu} was greater than that of h_u. To substantiate this quantitatively and to verify the parabolic pattern of growth noted above, the mixing height growth rate dh/dt was examined at these sites. Individual growth rates were computed between consecutive observations for all cases, and mean growth rates were determined over one-hour intervals centered on each hour and half hour. Each mean value in Fig. 14 was computed from at least 30 values. The results indicate that the mixing height growth rate increased nearly linearly at the urban (solid line) and nonurban (dashed line) sites. Additionally, h_{nu} growth rates were indeed larger than those of h_u. However, dh/dt was expected to be relatively constant at the nonurban site. A constant growth rate means that the mixing height grows linearly with time. This has been documented when sensible heating dominates the evolution of a convective mixing layer below the nocturnal inversion (Tennekes, 1973). Therefore, another

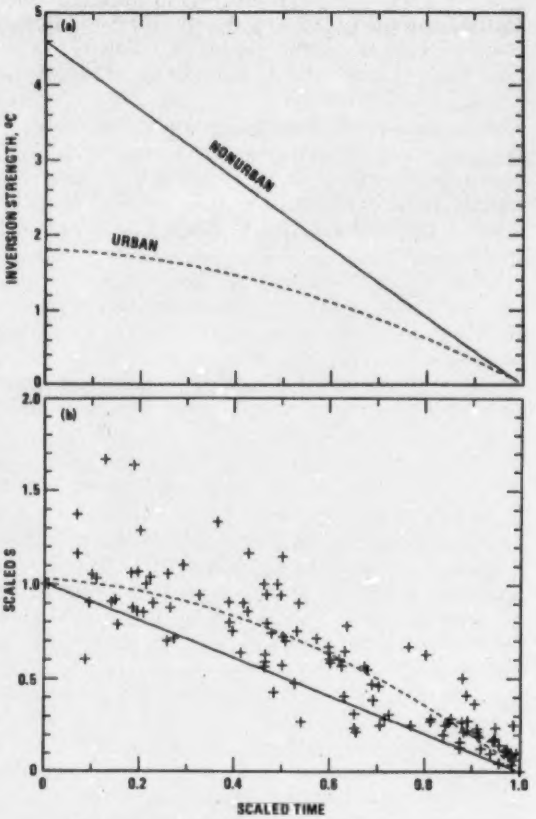

FIG. 17. a) Regression curves for the evolution of inversion strength (S) after sunrise at both sites and b) variation of scaled S at the urban (dashed line) and nonurban (solid line) site. The urban observations (pluses) are shown. Time has been scaled by the amount of time between sunrise and inversion erosion.

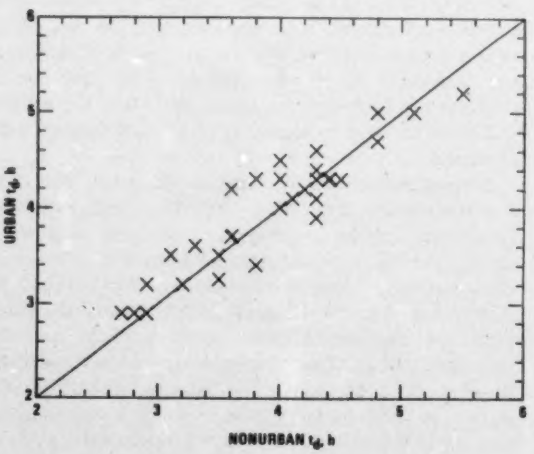

FIG. 16. Comparison of the amount of time, t_d, required to erode the nocturnal inversion at each site.

mechanism must be providing an additional contribution to mixing height growth.

Only minor variations in h_T are expected after sunrise if large-scale vertical motions or turbulent processes aloft are negligible. However, individual time histories indicated that h_T generally increased with time. A least-squares quadratic regression was applied to the observations at each site and the time-dependent variations are given by

$$h_{Tu} = 315.0 - 51.3t + 26.7t^2, \quad (6)$$

$$h_{Tnu} = 325.0 - 48.1t + 23.7t^2, \quad (7)$$

at the urban and nonurban sites, respectively. Larger variability of h_T was evident by an r of 0.74 and 0.66 for the urban and nonurban results, respectively. However, Eqs. (6) and (7) reveal that h_T followed the same evolutionary pattern and was essentially the same height at both sites. Since the relative change of h_T is of particular interest, the observations in Fig. 15 have been scaled by h_T at sunrise. The results

show that h_T exhibited an overall increase after sunrise, with the largest rises occurring later than two hours after sunrise. The variability in these results indicates that vertical motions probably differed among the cases. Nevertheless, the trend in h_T suggests that vertical motions were larger later in the morning. These results imply that greater convergence occurred later in the morning. Shreffler (1979b) reported that convergence was indeed larger during the day than at night. In addition, large variations in convergence were observed during the morning, which may explain some of the scatter exhibited in Fig. 15.

Vertical motion effects were accounted for by subtracting dh_T/dt from the actual mixing height growth rate to obtain a "relative" growth rate. Another method was to multiply dh_T/dt by the ratio h/h_T and then subtract the result from dh/dt. The factor h/h_T considers the possibility that vertical velocity is height dependent. The results showed smaller standard deviations for the second method while mean values were about 10% larger. The relative mixing height growth rates derived by the second method are denoted by the unconnected symbols in Fig. 14. The relative growth rate of h_{nu} was nearly constant. In fact, a mean dh_{nu}/dt of 3 cm s^{-1} was found from 1.5–4 h after sunrise. Relative h_u growth rates, on the other hand, were about half of the nonurban values for over 3 h after sunrise. During this period, the urban heat island was still relatively strong, although temperature differences between urban and rural locations became rapidly smaller as the environment outside the city warmed at a faster rate. Consequently, advective effects diminished with time. Ching *et al.* (1978) suggested that when horizontal temperature gradients disappear, heat flux is dominated by the local land use. Thus the relative growth rate of h_u in Fig. 14 increased and approached the nonurban value later in the morning. Another interesting result in Fig. 14 is that actual growth rates became increasingly larger than relative growth rates at both sites. This also suggests that vertical motions became greater with time.

Mixing height growth was greater than the rise of h_T, so the inversion layer became increasingly thinner and eventually eroded. Once the inversion completely eroded, rapid expansion of the mixing layer was often observed due to the weaker stability of the layer above h_T. It is useful to know when the nocturnal inversion erodes for mixing height models (Carson, 1973; Tennekes, 1973) and for air quality model applications. Time series of S were evaluated to determine the amount of time t_d from sunrise that was required to completely erode the nocturnal inversion. Individual least-squares quadratic regression curves fit the temporal behavior of S quite well during the morning because values of 0.96 and 0.98 were found in 31 cases at the urban and nonurban sites, respectively. There were an insufficient number of observations in four cases to determine t_d. In order to solve for t_d, S was set to zero in each regression equation. The interesting result was a mean t_d of 4.0 h at both sites. Hence, the inversion eroded about 0900 CST on an average basis. In addition, a standard deviation of 0.6 h was found with individual results ranging from 2.6–5.6 h. A comparison of individual results in Fig. 16 shows that t_d was about the same at each site, and that there was no evidence of a bias as a function of t_d. The largest difference in t_d between these sites was only about 0.3 h.

Since t_d varied by a factor of 2 among these cases, the temporal evolution of S for both sites is presented in Fig. 17 with the time difference between sunrise and an observation scaled by t_d. The curves in Fig. 17 were derived by least-squares regression fits to the urban and nonurban S observations. The larger S of the surface-based inversion decreased more rapidly than S at the urban site, which was continuously reinforced by advection of a stronger inversion during the morning. The urban observations in Fig. 17b were scaled by S at sunrise in each case to show that on several occasions S increased after sunrise at this site. The scaled values showed that the nonurban S diminished more rapidly as a fraction of its initial value whereas the rate of decrease of S at the urban site was more gradual.

8. Summary and conclusions

The evolution of the nocturnal inversion layer was investigated by analyses of observations derived from temperature profiles on fair weather summer evening and morning periods at an urban and a nonurban site. Nonurban inversion formation generally occurred within 1 h before sunset whereas formation was delayed by an average of 2.5 h after sunset at the urban site. Inversion growth at the nonurban site was more rapid before midnight with the overall evolution of h_T displaying a square root of time dependence. However, the growth of h_T at the nonurban site was also described quite well by a quadratic regression curve. After inversion formation at the urban site, the UBL height descended, except when there was a wind shift that resulted in a longer fetch upwind of the urban site.

Statistics of the inversion parameters at sunrise revealed that h_T was about the same height at both sites. The mean h_u at sunrise was 150 m at the urban site while the nonurban inversion was surface-based. The vertical temperature structure varied considerably with height at both sites. The nonurban temperature structure was most stable near the ground; however, an elevated peak in the temperature gradient was associated with the height of the nocturnal wind speed maximum. The temperature gradient in the UBL was approximately half of the dry adiabatic gradient; however, a trend toward even stronger stability with height of the UBL appeared. The greatest stability at the urban site was found near the middle of the elevated inversion.

Time histories of the mixing height observations after sunrise revealed that h_u and h_{nu} evolved in a parabolic manner. Mixing height growth rate statistics showed that h_{nu} increased faster than h_u. Consequently, by the time the inversion completely eroded, h_{nu} was about the same height as h_u. Advection of colder air and lower mixing heights is believed to have inhibited the growth rate of h_u. The urban mixing height growth curve is probably not applicable citywide since advective and vertical motion effects are believed to vary temporally and spatially. Both experimental (Ching *et al.*, 1978) and model (Barnum and Rao, 1975) results have shown that higher mixing heights and faster growth rates occur downwind of the urban heat island center after sunrise. The rise of h_T after sunrise indicated that the inversion layer was lifted. At the time the inversion was completely eroded, h_T was as much as three times higher than at sunrise. Vertical motions due to low-level convergence in the urban area are believed to be responsible for upward motions that produced a linear increase in the mixing height growth rate at both sites. When the variation in h_T was removed from the actual dh/dt, the growth rate of h_{nu} was nearly constant at 3 cm s^{-1}, while the growth rate of h_u was only about half as large as the nonurban value during most of the morning. The time for the inversion to erode at these sites coincided both on average and in individual cases. The mean amount of time for the inversion to be completely eroded was 4 h after sunrise.

REFERENCES

Ackerman, B., N. Westcott and P. H. Hildebrand, 1981: Diurnal cycle of the structure of the PBL over a metropolitan area. *Preprints, Fifth Symp. on Turbulence Diffusion and Air Pollution,* Atlanta, Amer. Meteor. Soc., 175–176.

Andre, J. C., and L. Mahrt, 1982: The nocturnal surface inversion and influence of clear-air radiative cooling. *J. Atmos. Sci.*, **39,** 864–878.

Anfossi, D., P. Bacci and A. Longhetto, 1974: An application of lidar technique to the study of the nocturnal radiation inversion. *Atmos. Environ.*, **8,** 537–541.

Arya, S. P. S., 1981: Parameterizing the height of the stable atmospheric boundary layer. *J. Appl. Meteor.*, **20,** 1192–1202.

Auer, A., 1978: Correlation of land use and cover with meteorological anomalies. *J. Appl. Meteor.*, **17,** 636–643.

Baker, D. G., J. W. Enz and H. J. Paulus, 1969: Frequency, duration, commencement time and intensity of temperature inversion at St. Paul–Minneapolis. *J. Appl. Meteor.*, **8,** 747–753.

Barnum, D. C., and G. V. Rao, 1975: Role of advection and penetrative convection in affecting the mixing height variations over an idealized metropolitan area. *Bound.-Layer Meteor.*, **8,** 497–514.

Bornstein, R. D., 1968: Observations of the urban heat island effect in New York City. *J. Appl. Meteor.*, **7,** 575–582.

Carson, D. J., 1973: The development of a dry inversion-capped convectively unstable boundary layer. *Quart. J. Roy. Meteor. Soc.*, **99,** 450–467.

Ching, J. K. S., J. F. Clarke and J. M. Godowitch, 1978: The variability of the heat flux and mixed layer depth over St. Louis, MO. *WMO Symp. Boundary Layer Physics Applied to Special Problems of Air Pollution.* WMO No. 510, Geneva, 71–78.

Clarke, J. F., 1969: Nocturnal urban boundary layer over Cincinnati, Ohio. *Mon. Wea. Rev.*, **97,** 582–589.

DeMarrais, G. A., 1961: Vertical temperature difference observed over an urban area. *Bull. Amer. Meteor. Soc.*, **42,** 548–554.

Duckworth, F. S., and J. S. Sandberg, 1954: The effect of cities upon horizontal and vertical temperature gradients. *Bull. Amer. Meteor. Soc.*, **35,** 198–207.

Godowitch, J. M., 1982: Diurnal variations in the vertical distribution of aerosol scattering coefficients over St. Louis, Mo. *Preprints, Third Joint Conf. Applications of Air Pollution Meteorology,* San Antonio, Amer. Meteor. Soc.

Hjelmfelt, M. R., 1982: Numerical simulation of the effects of St. Louis on mesoscale boundary layer airflow and vertical air motion: Simulations of urban vs nonurban effects. *J. Appl. Meteor.*, **21,** 1239–1257.

Kloppel, M., G. Stilke and C. Wamser, 1978: Experimental investigations into variations of ground-based inversions and comparisons with results of simple boundary layer models. *Bound.-Layer Meteor.*, **15,** 135–145.

Mahrt, L., R. C. Heald, D. H. Lenshcow, B. B. Stankov and I. Troen, 1979: An observational study of the structure of the nocturnal boundary layer. *Bound.-Layer Meteor.*, **17,** 247–264.

McElroy, J. L., 1973: A numerical study of the nocturnal heat island over a medium-size mid-latitude city (Columbus, Ohio). *Bound.-Layer Meteor.*, **3,** 442–453.

Moses, H., 1974: Argonne urban–rural airflow program. *Bull. Amer. Meteor. Soc.*, **56,** 112–114.

Oke, T. R., 1979: Review of urban climatology, 1973–1976. Techn. Note No. 169, WMO No. 539, 100 pp.

——, 1982: The energetic basis of the urban heat island. *Quart. J. Roy. Meteor. Soc.*, **108,** 1–24.

——, and C. East, 1971: The urban boundary layer in Montreal. *Bound.-Layer Meteor.*, **1,** 411–437.

——, and G. B. Maxwell, 1975: Urban heat island dynamics in Montreal and Vancouver. *Atmos. Environ.*, **9,** 191–200.

Pooler, F., 1974: Network requirements for the St. Louis regional pollution study. *J. Air Poll. Control Assoc.*, **24,** 228–231.

Schiermeier, F. A., 1978: Air pollution milestones: RAPS field measurements. *Environ. Sci. Technol.*, **12,** 644–651.

Shreffler, J. H., 1978: Detection of centripetal heat island circulations from tower data in St. Louis. *Bound.-Layer Meteor.*, **15,** 229–242.

——, 1979a: Urban–rural differences in tower-measured winds, St. Louis. *J. Appl. Meteor.*, **18,** 829–835.

——, 1979b: Heat island convergence in St. Louis during calm periods. *J. Appl. Meteor.*, **18,** 1512–1520.

Stull, R. B., 1983: Integral scales for the nocturnal boundary layer. Part 1: Empirical depth relationships. *J. Climate Appl. Meteor.*, **22,** 673–686.

Summers, P. W., 1965: An urban heat island model: Its role in air pollution problems with applications to Montreal. *First Canadian Conf. on Micrometeorology.* Toronto, CMOS, 22 pp.

Takle, E. S., R. H. Shaw and H. C. Vaugh, 1976: Low-level stability and pollution trapping potential for a rural area. *J. Appl. Meteor.*, **15,** 36–42.

Taylor, G. I., 1915: Eddy motion in the atmosphere. *Philos. Trans. R. Soc. London,* Series A, **215,** 26 pp.

Tennekes, H., 1973: A model for the dynamics of the inversion above the convective boundary layer. *J. Atmos. Sci.*, **30,** 558–567.

Yamada, T., 1979: Prediction of the nocturnal surface inversion height. *J. Appl. Meteor.*, **18,** 526–531.

Yap, D., K. Gunn and C. East, 1969: Vertical temperature distribution over Montreal. *Nat. Can.*, **96,** 561–580.

Yu, T., 1978: Determining height of the nocturnal boundary layer. *J. Appl. Meteor.*, **17,** 28–33.

NOTICE

This document has been reviewed in accordance with U.S. Environmental Protection Agency policy and approved for publication. Mention of trade names or commercial products does not constitute endorsement or recommendation for use.

This article documents research that was conducted under the auspices of the U.S. Environmental Protection Agency (USEPA). As an arm of the government, the USEPA has a paid up, non-exclusive, irrevocable, worldwide license to reproduce, prepare derivative works, and distribute to the public all of the material contained herein, and to others acting on its behalf the right to do so. The USEPA grants to the National Technical Information Service, Department of Commerce, the right to act as its agent in the distribution of this material.